SUPPLEMENTAL DATA

Supplementary Experimental Procedures

Fluorescence Microscopy - A Zeiss Axiovert 200M microscope equipped with a Zeiss 100x Plan-Apochromat (1.40 NA) DIC objective and Hamamatsu Orca 2 CCD camera was used to capture fluorescence images of yeast cells expressing Cdc34-GFP (Invitrogen) (1). Data was collected and analyzed with Zeiss Axiovision 4.6. Images were cropped and adjustments to brightness were made within Axiovision 4.6.

Zeiss Axiovision 4.6 with quantification module was used to measure mean pixel intensity. Circles of interest were drawn within the nucleus or cytoplasm. Background light was measured by selecting a large circle of interest outside of each cell. Mean pixel intensities (arbitrary units) were calculated by subtracting background from nuclear and cytoplasmic values.

Estimating the nuclear concentration of yeast Cdc34 - To estimate the nuclear concentration of yeast Cdc34 in haploid yeast cells, the number of Cdc34 molecules per cell was estimated by serially diluting known quantities of purified, bacterially-expressed Cdc34-Δ270 into an extract of *CDC34-myc* cells in which the genomic locus that encoded Cdc34 was modified by addition of sequences that encoded a myc epitope tag (RJD982). The tagged Cdc34 migrated slower than untagged bacterially-derived Cdc34-Δ270, which allowed us to distinguish the two species by SDS-PAGE. By immunoblotting with anti-Cdc34, scanning the film, and quantifying the resulting file with NIH Image, we estimated the endogenous protein to be present at 78,000 molecules/cell.

The ratio of nuclear and cytoplasmic Cdc34 was estimated by fluorescence microscopy of cells in which the genomic copy of *CDC34* was tagged with sequences that encode GFP. The average value for this ratio from 20 cells was 3.5 ± 0.6.

The average total volume of a haploid yeast cell was estimated at 42 fL (2,3). The total volume of the following organelles was also estimated: endoplasmic reticulum 0.7 fL, mitochondria 2.3 fL, vacuole 1.9 fL, and nucleus 2.6 fL (3). Given these values, the volume of cytoplasm was estimated from equation 1:

$$42\,fL - \sum organelles = 34.5\,fL \qquad (1)$$

Given these values, equation 2 derives the number of molecules in the nucleus and in the cytoplasm:

$$3.5X \times 0.07 + X \times 0.93 = 78{,}000 \qquad (2)$$

where 0.07 is the fractional volume of the nucleus and 0.93 is the fractional volume of the cytoplasm. Therefore X = 66,383, and the number of molecules of Cdc34 in the nucleus is 16,264. This was then divided by the respective volumes of the cytoplasm and nucleus and Avogadro's number to arrive at an estimate of ~ 10μM for the nuclear and 2.9 μM for the cytoplasmic concentration of yeast Cdc34.

GST pull-down binding assay – 2 nmole of either GST alone or GST-HACT were incubated in the presence of 30 ul of glutathione-sepharose 4B resin at 4°C for 1 hour. The beads were briefly incubated twice with wash buffer containing 30 mM Tris, pH 7.5, 100 mM NaCl, 0.1 % IgePal, 1 mM DTT and 5 % glycerol. Beads were then incubated with either Cul1–Rbx1 (80, 40, 20, 10, or 5 pmole) or a buffer only control at 4°C for 1 hour. The beads were washed twice with 1 ml of wash buffer and followed by the addition of 100 ul of 1X SDS-PAGE buffer. These reactions were boiled for 5 minutes and then used for analysis by SDS-PAGE.

The amount of Cul1–Rbx1 bound to the beads was determined by Western blot analysis with a monoclonal Cul1 antibody (Zymogen) and by comparison with known amounts of Cul1–Rbx1. Quantitative Western analysis was performed using an Alexa Fluor 680 goat anti-mouse IgG antibody (Molecular Probes) and the Odyssey infrared imaging system (Li-Cor Biosciences).

Neddylation of Cul1+Rbx1 and Cul1–Cdc34-WT and Cul1–Cdc34-Δ190 fusions - 600 nM Cul1+Rbx1 or Cul1 fusion proteins were incubated in the presence of 125 nM Nedd8 E1 (4), 0.5 μM Ubc12, 1 μM Nedd8 and 2 mM ATP at 20-22°C for 20 minutes. Neddylation was confirmed by Western blot analysis using a monoclonal Cul1 antibody (data not shown).

REFERENCES

1. Huh, W. K., Falvo, J. V., Gerke, L. C., Carroll, A. S., Howson, R. W., Weissman, J. S., and O'Shea, E. K. (2003) *Nature* **425**, 686-691
2. Jorgensen, P., Nishikawa, J. L., Breitkreutz, B. J., and Tyers, M. (2002) *Science* **297**, 395-400
3. Perktold, A., Zechmann, B., Daum, G., and Zellnig, G. (2007) *FEMS Yeast Res* **7**, 629-638
4. Huang, D. T., Schulman, B. A., and Raymond, J. D. (2005) Expression, Purification, and Characterization of the E1 for Human NEDD8, the Heterodimeric APPBP1-UBA3 Complex. in *Methods in Enzymology*, Academic Press. pp 9-20

Supplementary Figure Legends

Fig S1. Multiple sequence alignment of yeast Cdc34, human Cdc34a and Cdc34b, yeast Ubc8 and yeast Rad6 amino acid sequences. Residues encompassing the ubiquitin conjugating catalytic domain are shaded in pink. The human acidic tail residues and the yeast ones that are aligned to them are shaded purple. The residues in the yeast tail that extend beyond the human Cdc34 tail sequences are shaded green.

Fig S2. Yeast Cdc34-Δ230 and Cdc34-Δ270 have comparable activities when assayed with SCF and Sic1. Reactions containing 1.6 μM yeast E1, 100 nM yeast SCF, 1.2 μM ^{32}P-labeled Sic1, 100 nM yeast Cdc34-Δ230 or Cdc34-Δ270, and 150 μM ubiquitin were incubated for 2, 4, 6, 8 and 10 minutes prior to quenching with reducing SDS-PAGE buffer. Note that the Cdc34 concentration was within the k_{cat}/K_m range for both constructs which would maximize any potential differences in activity between the two Cdc34 proteins. The percentage of Sic1 substrate that was converted to product is given at the top of the gel for each time point. The differences observed between Cdc34-Δ230 and Cdc34-Δ270 are well within experimental error.

Fig S3. (A) Anti-Cdc34 Western blot of normalized extracts (12.5 μg/lane) from yeast strains sustained by either Cdc34-mycHIS6 protein (RJD982; lanes 1, 3-6) or un-tagged Cdc34 protein (RJD379; lane 2). Lanes 3-6 contain RJD982 extract mixed with either 1 ng (lane 3), 2 ng (lane 4), 4 ng (lane 5), or 8 ng (lane 6) of recombinant Cdc34-Δ270 protein. Lanes 7 and 8 contain only recombinant Cdc34-Δ270 protein (2 and 4 ng, respectively). (B) The Intensity of Cdc34-GFP fluorescence inside the nucleus (red circle nearest the center of the cell) and inside the cytoplasm (red circle adjacent to the cell wall) was determined. Left: representative DIC images for wild type cells expressing Cdc34-GFP from the endogenous locus. Middle: Cdc34-GFP localizes to the nucleus. Right: Red circles define areas for which mean pixel intensity was calculated. White bars: 2 μm.

Fig S4. Graph plotting the rate of Sic1 ubiquitylation against the concentration of Cdc34 acidic tail truncation proteins. The data were fit to the Michaelis-Menten equation using non-linear curve fitting (Prism). (A) Cdc34-Δ190. (B) Cdc34-Δ225. (C) Cdc34-Δ220. (D) Cdc34-Δ210. (E) Cdc34-Δ205. Each graphical data point represents the mean of duplicate data values from 2 independent experiments and the error bars are the standard deviation.

Fig S5. The human acidic tail domain is sufficient for binding to human SCF. (A) 2 nMole of either GST or a GST fusion of the human acidic C-terminal tail domain (GST-HACT) were immobilized on glutathione beads. Beads were then incubated in the presence of either 80 (lanes 2 and 8), 40 (lanes 3 and 9), 20 (lanes 4 and 10), 10 (lanes 5 and 11) or 5 (lanes 6 and 12) pMole of human Cul1–Rbx1 or in the presence of buffer as a negative control (lanes 1 and 7). Samples were then prepared as noted in the Experimental Procedures section above. To demonstrate even loading of GST and GST-HACT, 10 ul of each sample was loaded onto a 16 % SDS-PAGE gel and stained with coomassie blue Safe Stain (Invitrogen). Because Cul1 is expressed as two fragments, the NTD and CTD, these two fragments co migrate by SDS-PAGE and only one band is visible at the apparent MW of ~ 40 kDa. (B) Western blot of a 2-fold dilution series of Cul1–Rbx1. Intensities of the individual bands were quantified using Li-Cor Biosciences software and used to create a standard curve. The standard curve was used to quantify the amount of protein bound to the glutathione-sepharose beads and to generate the plot in Figure S4C. (C) Quantification of the GST pull-down experiment demonstrated specific binding between GST-HACT and Cul1–Rbx1 in a dose dependent manner. The statistical significance of the greater binding of Cul1–Rbx1 to GST-HACT than to GST alone was demonstrated using the unpaired Student's t test with Welch's correction (P-value < 0.01).

Fig S6. Neddylation of both Cul1–Cdc34-WT and Cul1–Cdc34-Δ190 fusion proteins has a stimulatory effect similar to the un-fused proteins. Di-ubiquitin synthesis assays comparing (A) wild-type and (B) Cdc34-Δ190 in the presence of either Cul1+Rbx1 or $Cul1^{Nedd8}$+Rbx1 or comparing (A) Cul1–Cdc34-WT and $Cul1^{Nedd8}$–Cdc34-WT or (B) Cul1–Cdc34-Δ190 and $Cul1^{Nedd8}$–Cdc34-Δ190. Reactions containing either 300 nM Cul1+Rbx1 and 300 nM Cdc34 or containing 300 nM Cul1–Cdc34 fusion, 0.7 μM human E1, 6 μM ^{32}P-labeled K48R ubiquitin, and 50 μM D77 ubiquitin were incubated at 20-22°C for the specified times and quenched with SDS-PAGE buffer. Note that neddylated Cul1–Cdc34-WT migrated at approximately the same apparent MW as the E1~Ub and was therefore obscured from view, whereas neddylated Cul1–Cdc34-Δ190~Ub was easily identified between the un-neddylated Cul1–Cdc34-Δ190~Ub species and E1~Ub (from this we were able to estimate the efficiency of the neddylation reaction at approximately 50 %). Also note that thioester formation for the Cul1–Cdc34-WT and $Cul1^{Nedd8}$–Cdc34-WT fusions was abnormally low in this experiment which resulted in the lower than normal activity of this protein.

Table S1. Statistics for the bioinformatics analysis of the yeast proteome.

Window	Percent	ORFs	Rand1	Rand2	Rand3	Average	σ
15	0.6	656	70.7	71.4	72.4	71.5	0.7
15	0.7	225	1.8	2.3	2.7	2.27	0.37
15	0.8	146	0.2	0.3	0.2	0.23	0.05
16	0.6	445	24.3	24.4	26.3	25	0.92
16	0.7	176	0.5	0.8	0.7	0.67	0.12
16	0.8	108	0.1	0.2	0	0.1	0.08
17	0.6	326	6.7	8.3	9.5	8.17	1.15
17	0.7	209	1.4	1	2	1.47	0.41
17	0.8	88	0	0.1	0.1	0.07	0.05
18	0.6	388	14.4	15.4	15.6	15.13	0.52
18	0.7	161	0.9	0.4	0.2	0.5	0.29
18	0.8	71	0	0	0	0	0
19	0.6	298	5.6	4.6	6.2	5.47	0.66
19	0.7	128	0.2	0.4	0.3	0.3	0.08
19	0.8	63	0	0	0	0	0
20	0.6	341	10.4	9.9	11.1	10.47	0.49
20	0.7	139	0.6	0.6	0.4	0.53	0.09
20	0.8	73	0	0	0.1	0.03	0.05
21	0.6	259	3.5	4.9	3.2	3.87	0.74
21	0.7	117	0.1	0.4	0.1	0.2	0.14
21	0.8	59	0	0	0	0	0
22	0.6	191	2.1	1.1	1.2	1.47	0.45
22	0.7	96	0	0.1	0	0.03	0.05
22	0.8	48	0	0	0	0	0
23	0.6	223	3	2.5	1.9	2.47	0.45
23	0.7	84	0	0.1	0	0.03	0.05
23	0.8	41	0	0	0	0	0
24	0.6	166	0.7	1.4	1.4	1.17	0.33
24	0.7	95	0.1	0	0.1	0.07	0.05
24	0.8	32	0	0	0	0	0
25	0.6	195	2.4	1.8	1.9	2.03	0.26
25	0.7	83	0.1	0	0	0.03	0.05
25	0.8	40	0	0	0	0	0

Window: number of residues within the search window. Percent: minimum percentage of residues within the window that must be acidic. ORFs: the number of yeast Open Reading Frames with at least one stretch of residues that satisfy the previous two conditions. Rand1, Rand2, and Rand3: Expected number of ORFs if amino acid sequences are shuffled from three

independent randomizations. Average: the average expected value from Rand1, Rand2, and Rand3. σ: the standard deviation for the expected values from Rand1, Rand2 and Rand3.

Figure S1

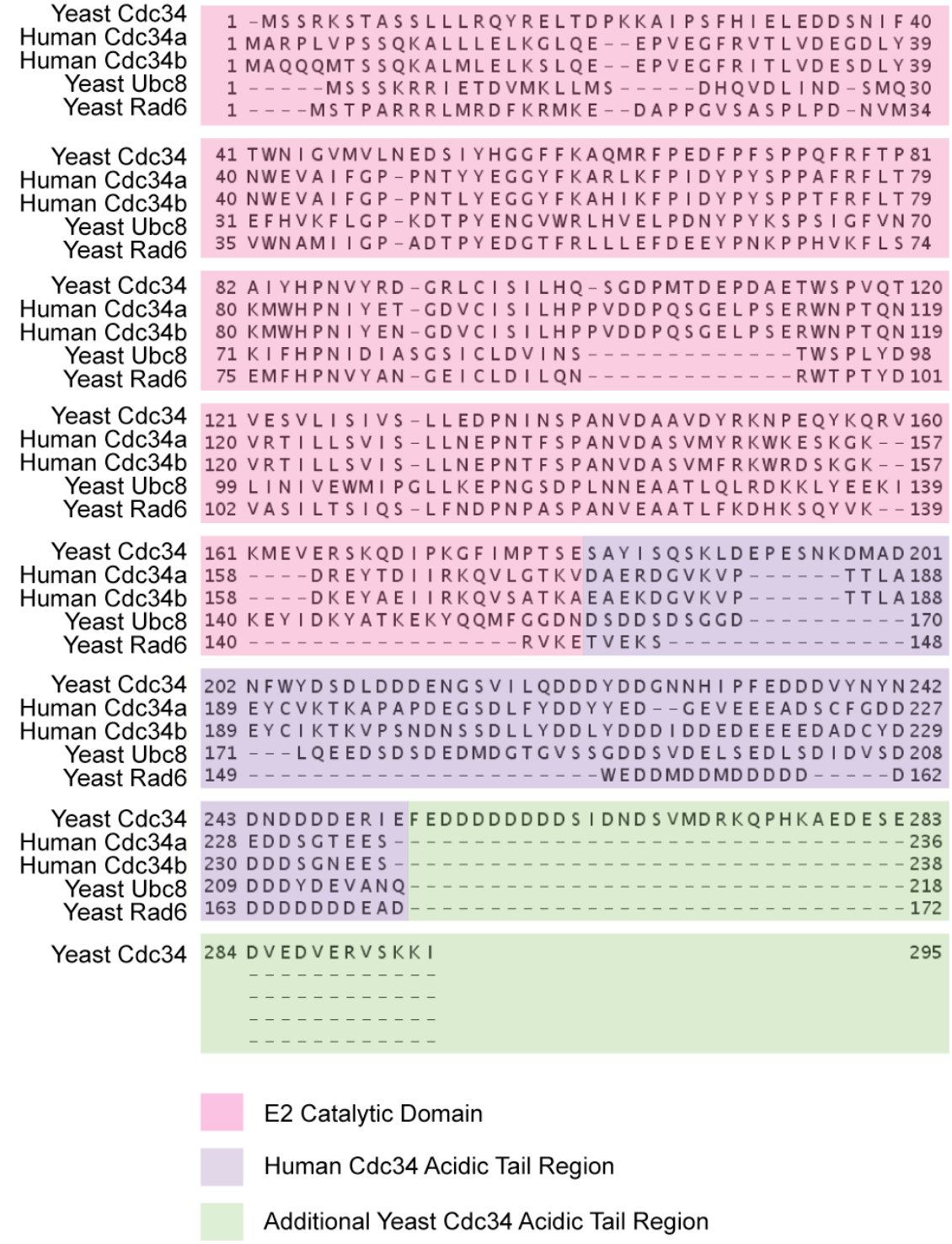
Yeast Cdc34
Human Cdc34a
Human Cdc34b
Yeast Ubc8
Yeast Rad6
1 -MSSRKSTASSLLLRQYRELTDPKKAIPSFHIELEDDSNIF 40
1 MARPLVPSSQKALLLELKGLQE--EPVEGFRVTLVDEGDLY 39
1 MAQQQMTSSQKALMLELKSLQE--EPVEGFRITLVDESDLY 39
1 -----MSSSKRRIETDVMKLLMS-----DHQVDLIND-SMQ 30
1 ----MSTPARRRLMRDFKRMKE--DAPPGVSASPLPD-NVM 34
41 TWNIGVMVLNEDSIYHGGFFKAQMRFPEDFPFSPPQFRFTP 81
40 NWEVAIFGP-PNTYYEGGYFKARLKFPIDYPYSPPAFRFLT 79
40 NWEVAIFGP-PNTLYEGGYFKAHIKFPIDYPYSPPTFRFLT 79
31 EFHVKFLGP-KDTPYENGVWRLHVELPDNYPYKSPSIGFVN 70
35 VWNAMIIGP-ADTPYEDGTFRLLLEFDEEYPNKPPHVKFLS 74
82 AIYHPNVYRD-GRLCISILHQ-SGDPMTDEPDAETWSPVQT 120
80 KMWHPNIYET-GDVCISILHPPVDDPQSGELPSERWNPTQN 119
80 KMWHPNIYEN-GDVCISILHPPVDDPQSGELPSERWNPTQN 119
71 KIFHPNIDIASGSICLDVINS----------TWSPLYD 98
75 EMFHPNVYAN-GEICLDILQN----------RWTPTYD 101
121 VESVLISIVS-LLEDPNINSPANVDAAVDYRKNPEQYKQRV 160
120 VRTILLSVIS-LLNEPNTFSPANVDASVMYRKWKESKGK--157
120 VRTILLSVIS-LLNEPNTFSPANVDASVMFRKWRDSKGK--157
99 LINIVEWMIPGLLKEPNGSDPLNNEAATLQLRDKKLYEEKI 139
102 VASILTSIQS-LFNDPNPASPANVEAATLFKDHKSQYVK--139
161 KMEVERSKQDIPKGFIMPTSESAYISQSKLDEPESNKDMAD 201
158 ----DREYTDIIRKQVLGTKVDAERDGVKVP------TTLA 188
158 ----DKEYAEIIRKQVSATKAEAEKDGVKVP------TTLA 188
140 KEYIDKYATKEKYQQMFGGDNDSDDSDSGGD----------170
140 ----------RVKETVEKS----------148
202 NFWYDSDLDDDENGSVILQDDDYDDGNNHIPFEDDDVYNYN 242
189 EYCVKTKAPAPDEGSDLFYDDYYED--GEVEEEADSCFGDD 227
189 EYCIKTKVPSNDNSSDLLYDDLYDDDIDDEDEEEEDADCYD 229
171 ---LQEEDSDSDEDMDGTGVSSGDDSVDELSEDLSDIDVSD 208
149 ----------WEDDMDDMDDDDD-----D 162
243 DNDDDDERIEFEDDDDDDDDSIDNDSVMDRKQPHKAEDESE 283
228 EDDSGTEES-----------------------------236
230 DDDSGNEES-----------------------------238
209 DDDYDEVANQ-----------------------------218
163 DDDDDDDEAD-----------------------------172
284 DVEDVERVSKKI 295
E2 Catalytic Domain
Human Cdc34 Acidic Tail Region
Additional Yeast Cdc34 Acidic Tail Region

Figure S2

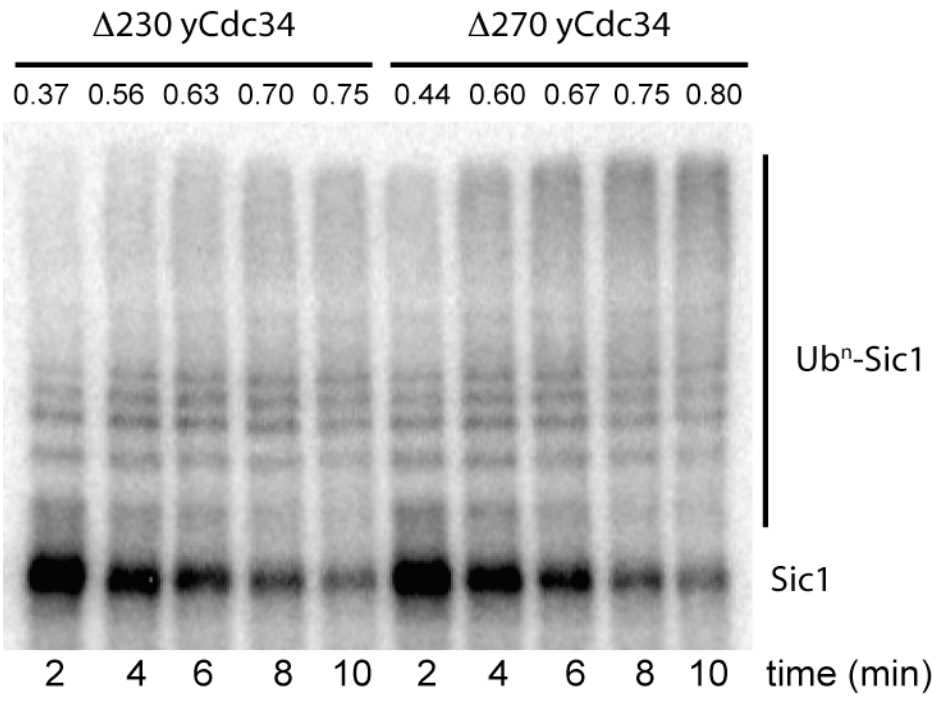
Δ230 yCdc34
Δ270 yCdc34
0.37 0.56 0.63 0.70 0.75 0.44 0.60 0.67 0.75 0.80
Ub^n-Sic1
Sic1
2 4 6 8 10 2 4 6 8 10 time (min)

Figure S3

A

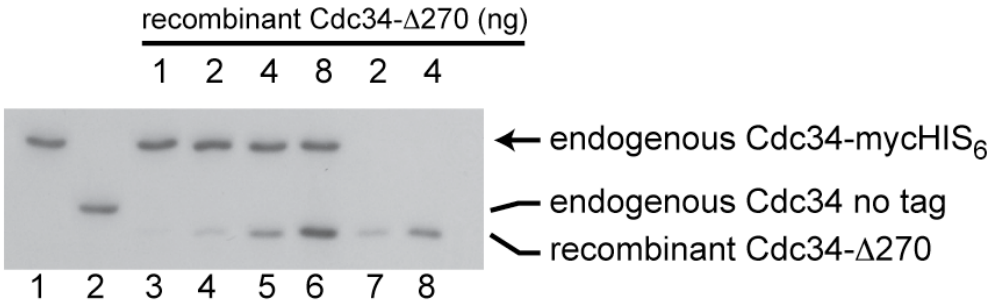
recombinant Cdc34-Δ270 (ng)
1 2 4 8 2 4
endogenous Cdc34-mycHIS6
endogenous Cdc34 no tag
recombinant Cdc34-Δ270
1 2 3 4 5 6 7 8

B

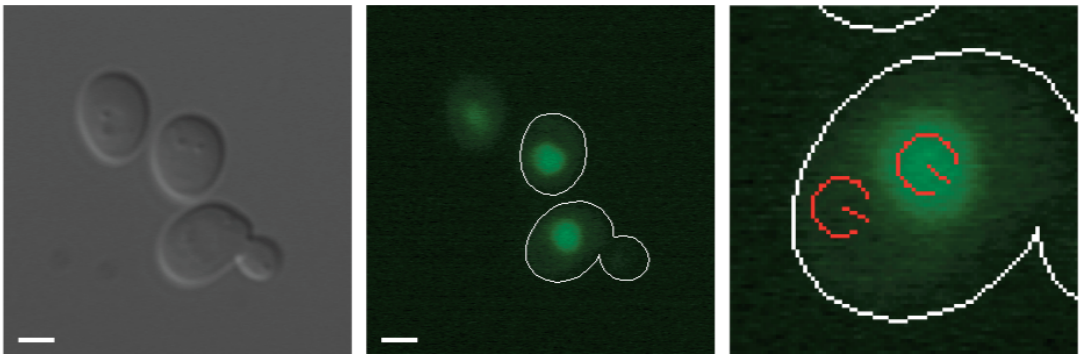

Figure S4

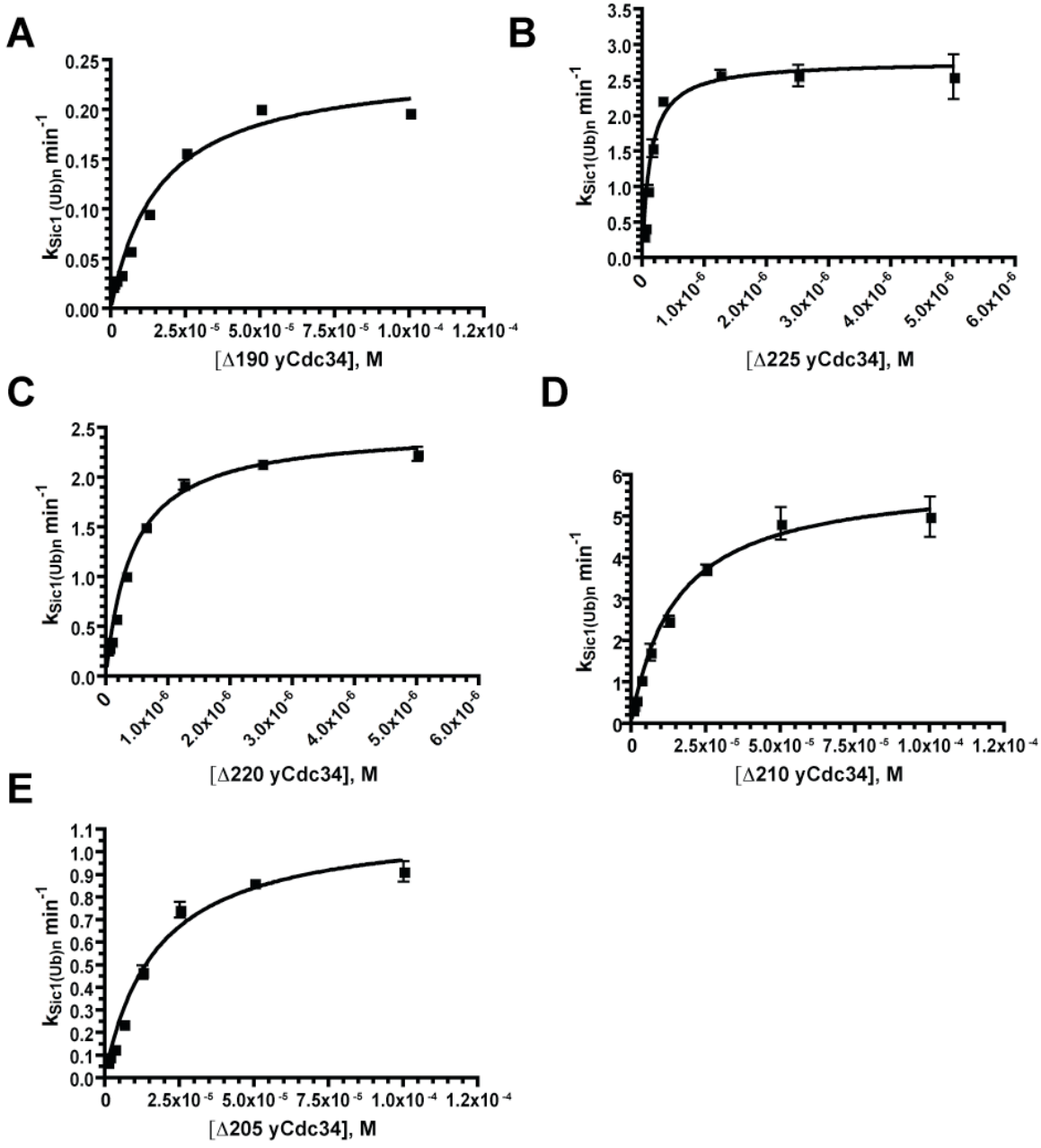
A
B
C
D
E
$k_{Sic1(Ub)n}$ min^{-1}
[Δ190 yCdc34], M
[Δ225 yCdc34], M
[Δ220 yCdc34], M
[Δ210 yCdc34], M
[Δ205 yCdc34], M

Figure S5

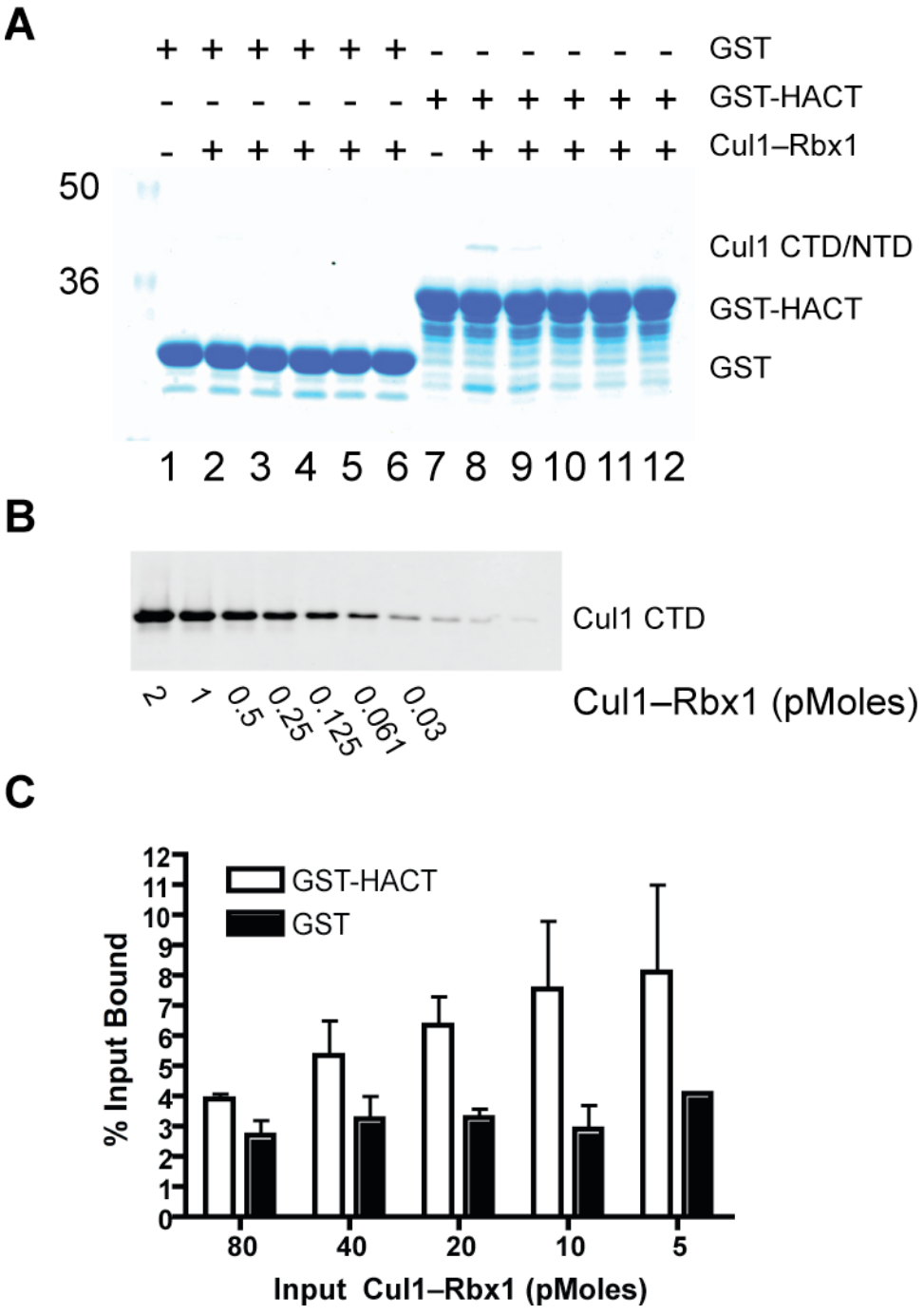
A
+ + + + + + - - - - - - GST
- - - - - - + + + + + + GST-HACT
- + + + + + - + + + + + Cul1–Rbx1
50
36
Cul1 CTD/NTD
GST-HACT
GST
1 2 3 4 5 6 7 8 9 10 11 12
B
Cul1 CTD
2 1 0.5 0.25 0.125 0.061 0.03
Cul1–Rbx1 (pMoles)
C
GST-HACT
GST
% Input Bound
0 1 2 3 4 5 6 7 8 9 10 11 12
80 40 20 10 5
Input Cul1–Rbx1 (pMoles)

Figure S6

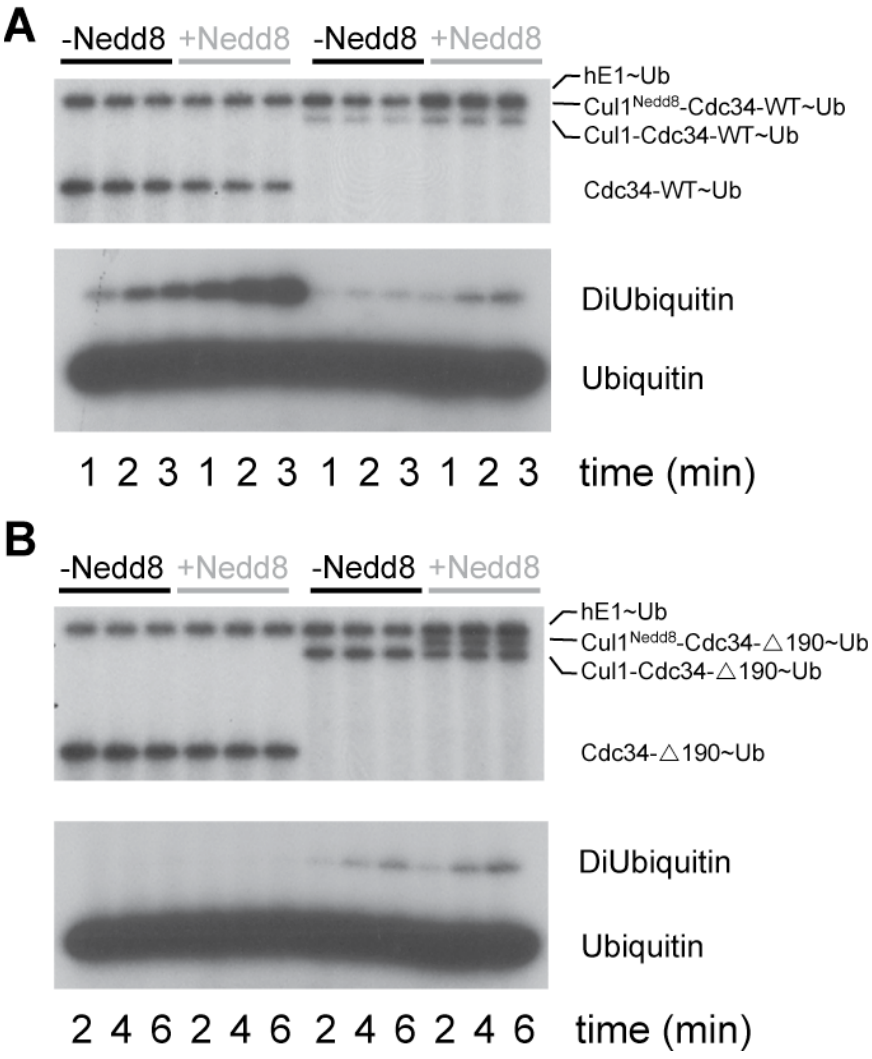
A
-Nedd8
+Nedd8
-Nedd8
+Nedd8
hE1~Ub
Cul1Nedd8-Cdc34-WT~Ub
Cul1-Cdc34-WT~Ub
Cdc34-WT~Ub
DiUbiquitin
Ubiquitin
1 2 3 1 2 3 1 2 3 1 2 3
time (min)
B
-Nedd8
+Nedd8
-Nedd8
+Nedd8
hE1~Ub
Cul1Nedd8-Cdc34-△190~Ub
Cul1-Cdc34-△190~Ub
Cdc34-△190~Ub
DiUbiquitin
Ubiquitin
2 4 6 2 4 6 2 4 6 2 4 6
time (min)